

Determination of Electrophoretic Mobility Distributions through the Analysis of Individual Mitochondrial Events by Capillary Electrophoresis with Laser-Induced Fluorescence Detection

Ciarán F. Duffy, Kathryn M. Fuller, Megan W. Malvey,[‡] Richard O'Kennedy,[†] and Edgar A. Arriaga*

Department of Chemistry, University of Minnesota, Minneapolis, Minnesota 55455

Here we report on the analysis of mitochondrial preparations by capillary electrophoresis with postcolumn laser-induced fluorescence detection. Individual mitochondria are detected by fluorescent labeling with the mitochondrion-selective probe, 10-nonyl acridine orange. Interactions between the organelles and the capillary walls are controlled by derivatization of the capillaries with poly-(acryloylaminopropanol). As expected from the presence of charged groups in their outer membranes, isolated mitochondria have intrinsic electrophoretic mobilities. This property may be influenced by variations in size, morphology, membrane composition, and damage caused during the isolation procedure. The mobility distributions of mitochondria isolated from NS1 and CHO cells ranged from -1.2×10^{-4} to $-4.3 \times 10^{-4} \text{ cm}^2 \text{ V}^{-1} \text{ s}^{-1}$ and -0.8×10^{-4} to $-4.2 \times 10^{-4} \text{ cm}^2 \text{ V}^{-1} \text{ s}^{-1}$, respectively. Furthermore, there seems to be no correlation between the density of the mitochondrial fraction and the resultant electrophoretic mobility distribution. These results suggest a new method for characterization of organelle fractions and for counting individual organelles.

Micrometer- and submicrometer-sized biological vesicles, such as organelles, microsomes formed during cell disruption, and artificial liposomes, have in common that they are defined by an outer phospholipid bilayer membrane.^{1–3} This membrane may contain protein and carbohydrate domains and may even include synthetic chemical groups in the case of liposomes. A variety of methods have been developed for the analysis and separation of these biological vesicles and other inorganic and organic colloidal particles.^{4,5} These methods include physical separations based on

sedimentation, size exclusion chromatography, and field flow fractionation. Electrophoretic properties that are dependent on the ζ potential, shape, size, and surface chemistry of the biological vesicles, and colloidal particles have also been the basis of several methods.^{4,6} These methods include free flow electrophoresis,⁷ gel electrophoresis,³ and capillary electrophoresis.⁴ Using the latter technique, methods to characterize polystyrene nanospheres,^{8,9} rat liver microsomes,³ and liposomes^{10–12} have been reported.

Most of the methods mentioned above will be adequate to describe sample parameters, such as the average and standard deviation of the vesicle property being measured; however, in many instances, it would be highly desirable to characterize individual vesicles or particles to better understand their behavior and to design superior analytical strategies. In the case of biological vesicles, flow cytometry has been exploited to determine properties of individual mitochondria. Because flow cytometry lacks a separation element, it is feasible to measure only those properties that can be determined from fluorescence or scattering, such as matrix volume,¹³ energy status,¹⁴ and membrane potential.^{15,16} Recently, we reported the electrophoretic mobility of individual liposomes, made by resuspension of dry phospholipids in an aqueous environment.¹⁷ Similarly, measurement of the electrophoretic mobility of each organelle would facilitate the evaluation of the dispersion of this property in a truly biological system.

To investigate the electrophoretic behavior of individual organelles, we have selected mitochondria as a model. These

* To whom correspondence should be addressed. E-mail: arriaga@chem.umn.edu.

[†] Current address: Ecolab Research Center, 840 Sibley Memorial Highway, Minneapolis, St. Paul, MN 55118.

[‡] Current address: School of Biotechnology, Dublin City University, Glasnevin, Dublin 9, Ireland.

(1) Sadava, D. E. *Cell Biology. Organelle Structure and Function*; Jones and Bartlett Publishers: Boston, 1993.

(2) Janoff, A. S.; Marcel Dekker: New York, 1999; p 451.

(3) Radko, S.; Sokoloff, A. V.; Garner, M. M.; Andreas, C. *Electrophoresis* **1995**, *16*, 981–992.

(4) Radko, S. P.; Chrambach, A. *J. Chromatogr. B* **1999**, *722*, 1–10.

(5) Hunter, R. J. *Foundations of Colloid Science*, 2nd ed.; Oxford University Press: Oxford, 2001.

(6) Jones, M. N. *Adv. Colloid Interface Sci.* **1995**, *54*, 93–128.

(7) Pasquali, C.; Fialka, I.; Huber, L. A. *J. Chromatogr. B* **1999**, *722*, 89–102.

(8) Radko, S. P.; Stastna, M.; Chrambach, A. *Electrophoresis* **2000**, *21*, 3583–3592.

(9) VanOrman, G. L.; McIntire, J. J. *Microcolumn Sep.* **1989**, *1*, 289.

(10) Radko, S. P.; Stastna, M.; Chrambach, A. *Anal. Chem.* **2000**, *72*, 5955–5960.

(11) Roberts, M. A.; Locascio-Brown, L.; MacCrehan, W. A.; Durst, R. A. *Anal. Chem.* **1996**, *68*, 3434–3440.

(12) Tsukagoshi, K.; Okumura, Y.; Nakajima, R. *J. Chromatogr.* **1998**, *813*, 402–407.

(13) de Gannes, F. M. P.; Belaud-Rotureau, M. A.; Voisin, P.; Leducq, N.; Belloc, F.; Canioni, P.; Dolez, P. *Cytometry* **1998**, *33*, 333–339.

(14) Lopez-Medavilla, C.; Orfao, A.; Garcia, M. V.; Medina, J. M. *Biochim. Biophys. Acta, Bioenerg.* **1995**, *1232*, 27–32.

(15) Cossarizza, A.; Ceccarelli, D.; Masini, A. *Exp. Cell Res.* **1996**, *222*, 84–94.

(16) Petit, P. X.; O'Connor, J. E.; Grunwald, D.; Brown, S. C. *Eur. J. Biochem.* **1990**, *194*, 389–397.

(17) Duffy, C. F.; Gafoor, S.; Richards, D.; Admadzadeh, H.; O'Kennedy, R.; Arriaga, E. A. *Anal. Chem.* **2001**, *73*, 1855–61.

organelles generate ATP¹⁸ and are believed to play a key role in cell apoptosis.^{19,20} Mitochondrial malfunction has been linked to diseases^{21–23} and aging.^{24,25} A clear description of this linkage has been hampered by the coexistence of normal and abnormal mitochondria within the same cell. The description of mitochondrial enzymatic activity, protein maps, or response to pharmacological treatment may be equally biased by mitochondrial diversity. Direct visualization of labeled mitochondria in intact cells by confocal or electron microscopy provides insight into function and morphology.^{26–28} When properly labeled for identification, flow cytometry is also useful to determine mitochondrial properties within whole cells.^{29,30} Unfortunately, averaging the responses of the hundreds to thousands of mitochondria within a cell that are continually experiencing fusion and fission,^{31,32} or the millions of mitochondria present in isolates, hides the diversity of mitochondrial properties, likely compromising the interpretation of the data. The measurement of individual mitochondrial properties in an isolate or in a cell would provide an enhanced description of the role of mitochondria in cell function, disease, and aging.

Here, we demonstrate that capillary electrophoresis with postcolumn laser-induced fluorescence detection (CE-LIF) is useful in measuring the electrophoretic mobility of individual mitochondria isolated from Chinese hamster ovary cells (CHO) and NS1 mouse hybridoma cells. Mitochondria are fluorescently labeled with 10-nonyl acridine orange (NAO), which binds selectively to cardiolipin, a phospholipid synthesized and localized in the mitochondrial membranes. In addition to counting mitochondria, the distributions of individual mitochondrial electrophoretic mobilities are compared among the cell lines and between two mitochondrial fractions with different densities. The advantages of the bioanalytical strategy described here are likely to be useful in the characterization of other organelles, microsomes, or colloidal particles.

EXPERIMENTAL SECTION

Reagents. Sucrose, dimethyl sulfoxide (DMSO), and sodium tetraborate were purchased from Fisher Scientific (Pittsburgh, PA). *N*-[2-Hydroxyethyl]piperazine-*N*-[ethanesulfonic acid] (HEPES),

D-mannitol, ethylenediaminetetraacetic acid (EDTA), metrizamide (Mz), and Percoll (Pc) were purchased from Sigma (St. Louis, MO). CE buffers contained 10 mM borate, 10 mM sodium dodecyl sulfate (BS buffer), pH 9.3, or 250 mM sucrose, 10 mM HEPES (sucrose–HEPES buffer), pH 7.5, for separation of CHO-derived mitochondria and pH 7.39 for separation of NS1-derived mitochondria. The mitochondrial isolation buffer (M buffer) consisted of 210 mM D-mannitol, 70 mM sucrose, 5 mM HEPES, and 5 mM EDTA, adjusted to pH 7.35 with potassium hydroxide (Aldrich, Milwaukee, WI). All buffers were made with Milli-Q deionized water and filtered (0.2 μ m) prior to use. Stock solutions of 10^{-3} M fluorescein and 10^{-3} M 10-nonyl acridine orange (NAO) (Molecular Probes, Eugene, OR) were made in ethanol and DMSO, respectively. Dilutions of these solutions were prepared immediately prior to use. A 100 mg/mL digitonin (Aldrich) stock solution was prepared in DMSO and diluted to 10 mg/mL in M buffer before using.

Mitochondria Preparation. The mitochondria used in this study were isolated from CHO and NS1 cells grown at 37 °C and 5% CO₂. The CHO cells (a kind donation from Dr. Wei-Shou Hu, Department of Chemical Engineering, University of Minnesota) were cultured in 90% α -modified minimum essential medium (Eagle), 10% fetal bovine serum. The NS1 cells (a kind donation from Dr. Sally Palm, Department of Laboratory Medicine and Pathology, University of Minnesota) were cultured in 90% Dulbecco's Modified Eagle's Medium, 10% calf serum (all cell culture reagents were from Sigma). Cells were maintained by the addition of new media every 2–3 days. Biosafety level I was observed in all preparations.

A differential centrifugation protocol loosely based on procedures from Howell, et al.³³ and Bogenhagen, et al.³⁴ was followed to extract mitochondria from the NS1 cells. Briefly, NS1 cells in the log phase were washed three times with cold M buffer and counted using a Fuchs-Rosenthal hemacytometer (Hausser Scientific, Horsham, PA). Cells were diluted in M buffer to 8.6×10^6 cells/mL. To two 1.5-mL siliconized microcentrifuge tubes, 1-mL aliquots of the cell suspension and 2.5 μ L of 10 mg/mL digitonin solution were added. Following a 5-min incubation on ice, the tubes were placed in an ice-cooled cell disruption bomb (Parr Instrument Co., Moline, IL) that was charged with N₂ to 650 psi for 20 min. As estimated by light microscopy, 90% of the cells were disrupted. The mitochondria in one of the 1-mL aliquots of homogenate were labeled with 10 μ M NAO for 5 min. Whole cells, nuclei, and large cell debris were removed from the stained and unstained samples by centrifugation at 1400g for 5 min in an Eppendorf 5415D centrifuge, and the supernatants were removed and centrifuged again, for a total of three repetitions. The final supernatants were then centrifuged at 14000g for 20 min, and the pellets were resuspended in 0.5 mL of sucrose–HEPES buffer and kept on ice until analyzed.

A discontinuous gradient described by Madden, et al.³⁵ was used to isolate mitochondria from the CHO cells. The mitochondria were labeled with 10 μ M NAO for 5 min at room temperature while the cells were still intact. The mitochondria were isolated after NAO labeling was confirmed by fluorescence microscopy. Briefly, 2 mL of cell suspension (1×10^6 cells/mL) was

- (18) Cooper, G. M. *The Cell: A Molecular Approach*; ASM Press: Washington, DC, 1997.
- (19) Raha, S.; Robinson, B. H. *Am. J. Med. Genet.* **2001**, *106*, 62–70.
- (20) Golstein, P. *Science* **1997**, *275*, 1081–1082.
- (21) Shoffner, J. M.; Wallace, D. C. In *The Metabolic and Molecular Bases of Inherited Disease*; Scriver, C. R., Beaudet, A. L., Sly, W. S., Valle, D., Eds.; McGraw-Hill: New York, 1995; Vol. 1, pp 1535–1609.
- (22) Richard, S. M.; Bailliet, G.; Paez, G. L.; Bianchi, M. S.; Peltomaki, P.; Bianchi, N. O. *Cancer Res.* **2000**, *60*, 4231–4237.
- (23) Dimauro, S.; Schon, E. A. *Am. J. Med. Genet.* **2001**, *106*, 18–26.
- (24) Salvio, S.; Bonafe, M.; Capri, M.; Monti, D.; Franceschi, C. *FEBS Lett.* **2001**, *492*, 9–13.
- (25) Lesnfsky, E. J.; Gudiz, T. I.; Moghaddas, S.; Migita, C. T.; Ikeda-Saito, M.; Turkaly, P. J.; Hoppel, C. L. *J. Mol. Cell. Cardiol.* **2001**, *33*, 37–47.
- (26) Karbowski, M.; Kuroki, C.; Wozniak, M.; Ostrowski, M.; Teranishi, M.; Soji, T.; Wakabayashi, T. *Biochim. Biophys. Acta, Mol. Cell Res.* **1999**, *1449*, 25–40.
- (27) Serafino, A.; Sinibaldi-Vallebona, P.; Lazzarino, G.; Tavazzi, B.; Di Pierro, D.; Rasi, G.; Ravagnan, G. *Anticancer Res.* **2000**, *20*, 3383–3394.
- (28) Gilkerson, R. W.; Margineantu, D. H.; Capaldi, R. A.; Selker, J. M. *FEBS Lett.* **2000**, *474*, 1–4.
- (29) Leprat, P.; Ratinaud, M. H.; Julien, R. *Mech. Ageing Dev.* **1990**, *52*, 149–67.
- (30) Sureda, F. X.; Escubedo, E.; Gabriel, C.; Comas, J.; Camarasa, J.; Camins, A. *Cytometry* **1997**, *28*, 74–80.
- (31) Santel, A.; Fuller, M. T. *J. Cell Sci.* **2001**, *114*, 867–874.
- (32) Yoon, Y.; McNiven, M. A. *Curr. Biol.* **2001**, *11*, R67–R70.

(33) Howell, N.; Nalty, M. S.; Appel, J. *Plasmid* **1986**, *16*, 77–80.

(34) Bogenhagen, D.; Clayton, D. A. *J. Biol. Chem.* **1974**, *249*, 7991–7995.

(35) Madden, E. A.; Storrie, B. *Anal. Biochem.* **1987**, *163*, 350–357.

homogenized on ice using a Potter-Elvehjem tissue homogenizer. Homogenization was followed visually by light microscopy to ensure the use of a minimum number of strokes for disruption of 75% of the initial number of cells. The homogenate was centrifuged at 1300*g* for 5 min to remove nuclear and membranous material. The pellet was resuspended in ice-cold 250 mM sucrose and spun again; both supernatant fractions were combined to give a total post-nuclear supernatant (PNS).

A hybrid Pc/Mz discontinuous gradient was prepared using 250 mM sucrose in Labcor 16-mL ultracentrifugation tubes.³⁵ A volume of 2 mL of 35% Mz ($\rho = 1.1907$ g/mL) was overlaid with 2 mL of 17% Mz ($\rho = 1.1079$ g/mL), which in turn was overlaid with 5 mL of 6% Pc ($\rho = 1.0406$ g/mL). The PNS, total volume 1.7 mL, was gently overlaid. Centrifugation was carried out at 4 °C in a Beckman centrifuge (model J2-21) at 50000*g* for 15 min with the brake setting at zero. According to Madden, there are two interfaces that are enriched in mitochondria. The densest mitochondria (1.1079–1.1907 g/mL) are in the interface that is formed between the 17 and 35% Mz layers (Mz 17%/Mz 35%). The less dense mitochondria (1.0406–1.1079 g/mL) are in the interface that is formed between the 6% Pc and 17% Mz layers (Pc 6%/Mz 17%). The former interface is expected to contain mitochondria with minimum contamination from other organelles, but the latter interface, although containing a higher number of mitochondria, is not so pure. Following centrifugation, mitochondrial fractions from these interfaces were carefully removed using a blunt-ended needle and were kept on ice until analyzed.

Capillary Electrophoresis. The design and setup of the electrophoresis system with postcolumn laser-induced fluorescence detection used for this study was described previously.¹⁷ The 488-nm line from an argon-ion laser (Melles Griot, Irvine, CA) was used for excitation. Fluorescence emission was monitored spectrally using an interference filter transmitting in the range 522–552 nm (Omega Optical, Brattleboro, VT). To reduce scattering at 488 nm caused by interactions between the laser beam and mitochondria or air bubbles, an additional rejection band filter (488–53D, OD4, Omega Optical) was placed in front of the interference filter.

Separations were carried out using both poly(acryloylamino-propanol) (poly-AAP)-coated³⁶ and bare fused silica capillaries, 50 μ m i.d., 150 μ m o.d. The poly-AAP coating reduces the interactions between proteins associated with the outer mitochondrial membrane and the capillary wall. The detector alignment was optimized by continuously introducing a 10^{-9} M solution of fluorescein in BS or sucrose–HEPES buffer by electrokinetic pumping at -200 V cm⁻¹. Detector optimization was completed by observing the reproducibility of the fluorescence produced by individual 6- μ m fluorescently labeled latex beads (Molecular Probes, Eugene, OR). For mitochondrial analysis, the suspension was electrokinetically injected for 5 s at -50 V/cm and separated at -200 V/cm for CHO-derived mitochondria and injected for 5 s at -100 V/cm and separated at -200 V/cm for NS1-derived mitochondria. Sucrose–HEPES buffers were used in all separations.

Data Analysis. The output from the photomultiplier tube was electronically filtered (RC = 0.01 s) and then digitized using a PCI-MIO-16E-50 I/O board driven by Labview software (National

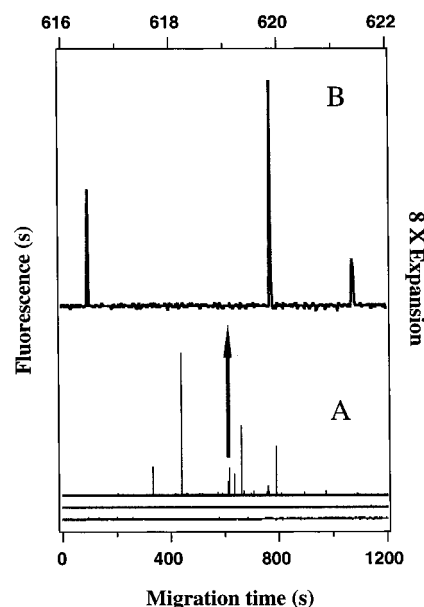


Figure 1. Capillary electrophoresis of mitochondria prepared from NS1 cells. Forty-seven spikes are present in the upper trace in part A resulting from the analysis of mitochondria isolated from cells treated with NAO. In part B, three spikes are better appreciated in the expansion of a 4-s migration time window, equivalent to the width of the arrow. The lower trace in part A is a control containing 10^{-5} M NAO alone. The middle trace in part A is a control containing mitochondria from cells that were not labeled with NAO. Samples were introduced electrokinetically for 5 s at -100 V cm⁻¹. Separations were performed at -200 V⁻¹ in a 27.4-cm 50- μ m i.d. poly-AAP-coated capillary in a 10 mM HEPES, 250 mM sucrose. Excitation, 488 nm argon line; detection, 522–552 nm.

Instruments, Austin, TX). The data were stored as binary files that were then analyzed using Igor Pro software (Wavemetrics, Lake Oswego, OR). Tabulation of peak intensities and migration times for individual events was performed using PickPeaks, an in-house-written Igor procedure that has been previously described.¹⁷ The program selects those events with signal intensities higher than 3 times the standard deviation of the background and the events are sorted in order of increasing intensity. A comparison among the sorted events from the mitochondrial electropherogram and the corresponding controls allows for selection of a new threshold that clearly identifies events corresponding to a migration time window in the mitochondrial electropherogram. The events in the migration time window are used to calculate individual electrophoretic mobilities.

RESULTS AND DISCUSSION

Mitochondria Analysis. An electropherogram resulting from the electrokinetic injection of a mitochondrial isolate from NS1 cells consists of spikes, as shown in the upper trace of Figure 1A. Instead of the typical migration zones observed in electropherograms of small ions or molecules, 47 spikes are detected (Figure 1A). As suggested in Figure 1B, an expansion of a 4-s migration time window from the upper trace of Figure 1A, all of the spikes have practically the same width, 200 ms. As expected, the peak width is the same whether the spike was detected early or late in the separation and depends on the traveling time through the tightly focused laser beam that defines the detection volume in the postcolumn laser-induced fluorescence detector. The charac-

(36) Gelfi, C.; Curcio, M.; Righetti, P. G.; Sebastiano, R.; Citterio, A.; Ahmadzadeh, H.; Dovichi, N. J. *Electrophoresis* **1998**, *19*, 1677–1682.

teristic peak width is one of the criteria for identification of a spike and exclusion of potential broad migration zones caused by free dye in the sample.

Identification of these spikes as individual mitochondrial species relies on the specificity of NAO, which forms a complex ($K_D = 6.6 \times 10^5 \text{ M}^{-1}$) with cardiolipin, a phospholipid specifically found in the mitochondrial inner membrane³⁷ and the use of a mitochondrial isolation procedure. As expected, the analysis of a control containing only NAO and no mitochondria, lower trace in Figure 1A, results in a spike-free electropherogram. Similarly, the electropherogram of unlabeled mitochondria, middle trace in Figure 1A, does not have spikes, indicating that scattering is not causing false spikes and that mitochondrial components do not have significant autofluorescence when excited with the 488-nm line of an argon-ion laser.

Although each detected event is likely caused by an individual mitochondrion, mitochondrial fragments or aggregates resulting from the disruption process may also be detected. To minimize the presence of fragments, we adopted nitrogen cavitation for cell disruption, because it is known that this procedure produces intact organelles, minimizing the chance of detecting fragments.^{38,39} No systematic studies of mitochondrial aggregation in isolation buffers have been reported; however, buffers relying primarily on mannitol for osmotic support are favored because, relative to sucrose, they exhibit decreased binding to glycogen.⁴⁰ The isolation buffer mimics the pH and osmolarity of the original cellular environment, minimizing the chances of agglomeration by retaining the electrostatic repulsions among mitochondria, which are negatively charged at biological pH.

The signal intensity of each mitochondrial species is also highly variable as seen in the upper trace of Figure 1A and in Figure 1B. Although the 2:1 stoichiometry in the NAO cardiolipin complex suggests that peak intensity is a measurement of cardiolipin content, there are several factors that make the fluorescence intensity a qualitative parameter: (i) For the CHO cells, the NAO concentration in the cytoplasm is expected to be different from the extracellular NAO concentration used for whole cell labeling and may also be variable within the cell. (ii) Determination of an appropriate concentration of NAO is not straightforward. In excess, NAO may stain other phospholipids found in the mitochondrial membranes, $K_D = 7 \times 10^4 \text{ M}^{-1}$ for phosphatidylserine and phosphatidylinositol;³⁷ in deficit it will not saturate the cardiolipin binding sites, thus prohibiting accurate determination of the total cardiolipin content. (iii) Variations in detector response as determined using fluorescently labeled latex beads may be as large as RSD = 35% (data not shown). Therefore, the fluorescence intensity is only a qualitative estimate of the amount of cardiolipin in a given mitochondrial species. Further work to quantitatively detect cardiolipin in individual mitochondria is in progress.

Despite its qualitative nature, signal intensity is a useful criterion to distinguish detected mitochondrial species from events

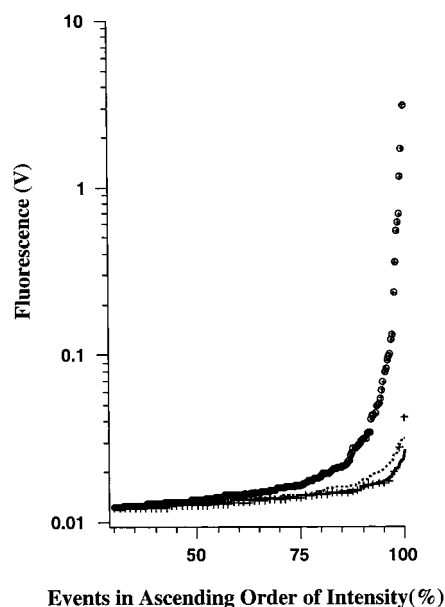


Figure 2. Events sorted in order of increasing intensity. All of those peak signals higher than 0.0114 V, a threshold equal to 3σ in the range 0–300 s are included. The percentage scale of the x axis facilitates comparison of regions with different numbers of events. Circles correspond to the mitochondrial electropherogram, upper trace, Figure 1A; the dotted line corresponds to unlabeled mitochondria, middle trace, Figure 1A; the solid line corresponds to the NAO control, lower trace, Figure 1A. The data above were all collected in the migration window 300–1170 s. The data marked with “+” correspond to the mitochondrial electropherogram, upper trace, Figure 1A, in the migration window 0–300 s.

caused by random background noise. Figure 2 shows the sorted intensities of the spikes present in the electropherograms of Figure 1A. Each electropherogram has a background standard deviation (σ) close to 0.0038 V (RSD 3.9%) in the range 0–300 s, a region where mitochondrial species are not detected. Only events with intensities larger than 3σ are included in Figure 2. High-intensity events are abundant only in the NAO-labeled mitochondrial electropherogram. The controls for unlabeled mitochondria (middle trace, Figure 1A) and NAO alone (lower trace, Figure 1A) collected over the range 0–1170 s resemble the events in the 0–300-s range of the NAO-labeled mitochondrial electropherogram. Alternatively, in all of the data sets, 60% of the sorted events have values lower than 0.013 V. These events are considered false positives and are expected from the statistical sampling if noise is described by a normal distribution. In this case, 0.3% of events will lie outside of 3σ . For example, considering the window 0–300 s (15 000 points), there should be 45 false positives, a number of the same magnitude as the actual number of false positives detected in the window. However, there are events in the 60 and 90% intensity range that could not be easily assigned to mitochondria or random events. Only those events with fluorescence higher than 0.037 V are unique to the NAO-labeled mitochondrial electropherogram. Additionally, Figure 2 suggests that most of the events in the controls and the premigration window (0–300 s) never reach 0.02 V, which is confirmed by a histogram distribution and appreciated as a plateau in Figure 2. Therefore, when drawing conclusions related to the analysis of mitochondrial species, we considered only those events with intensities higher than 0.02 V.

(37) Petit, J.-M.; Maftah, A.; Ratinaud, M. H.; Julien, R. *Eur. J. Biochem.* **1992**, *209*, 267–273.

(38) Hunter, M. J.; Commerford, S. L. *Biochim. Biophys. Acta* **1961**, *47*, 580–586.

(39) Adachi, S.; Gottleib, R. A.; Babior, B. M. *J. Biol. Chem.* **1998**, *273*, 19892–19894.

(40) Graham, J. M. In *Subcellular Fractionation A Practical Approach*; Graham, J. M., Rickwood, D., Eds.; IRL Press: New York, 1997; pp 1–29.

Table 1. Electrophoretic Mobility Distributions of Mitochondria^a

	NS1 Cells				CHO Cells
	1	2	3	ave \pm std dev ^b	ave \pm std dev ^b
range	-1.2 to -4.0	-1.2 to -4.3	-1.2 to -4.1	-1.2 to -4.3 ^c	-0.8 to -4.2 ^c
25th percentile	-1.8	-1.7	-1.4	-1.7 \pm 0.2	-1.2 \pm 0.2
median	-2.0	-2.1	-1.7	-1.9 \pm 0.2	-1.4 \pm 0.1
75th percentile	-2.7	-2.7	-2.9	-2.8 \pm 0.1	-1.7 \pm 0.2
total events	51	47	32	43 \pm 10	157 \pm 59

^a All values except total events are electrophoretic mobility values multiplied by 10^4 and given in units of $\text{cm}^2 \text{V}^{-1} \text{s}^{-1}$. ^b Average and the standard deviation of the value obtained from three replicates. Individual replicates are not shown for CHO cells. ^c Range for all of the events combined.

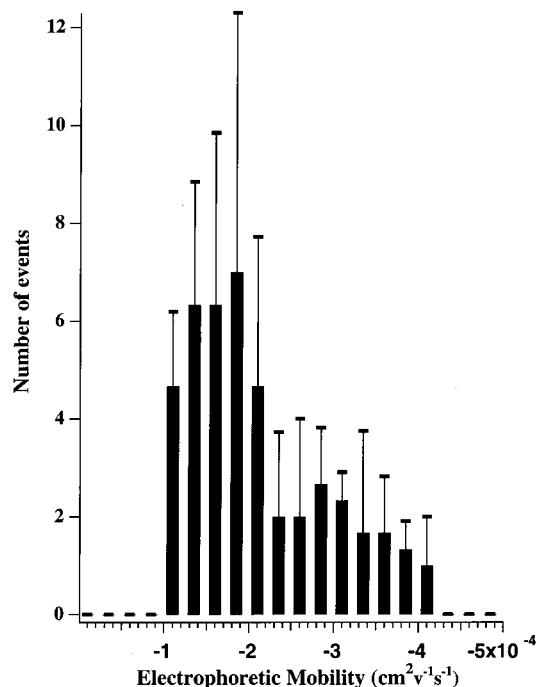


Figure 3. Electrophoretic mobility distribution. The migration time for detected events with signals higher than 0.02 V were used to calculate the electrophoretic mobility of the event. Bins are $0.225 \times 10^{-4} \text{ cm}^2 \text{V}^{-1} \text{s}^{-1}$ wide. The mitochondrial isolate was analyzed in triplicate. The height of the thick bar represents the average; the thin line represents one standard deviation. Other conditions as in Figure 1.

Analysis of NS1 mitochondria by CE-LIF, as described in Figure 1, was done in triplicate. The number of detected events with signals larger than 0.02 V was 43 ± 10 , Table 1. The variation in the number of events was not caused by heterogeneity in the isolate, because the sample was thoroughly mixed prior to injection. In addition, proper controls between consecutive electrophoretic separations confirmed that there was no carry over of mitochondria to the next separation. That the variation is slightly larger than expected from a Poisson distribution ($\sqrt{N} = 7$) may be the result of electrokinetic bias or anomalies in the sampling due to simultaneous introduction of a large number of mitochondria.

The combined results for three replicates of mitochondrial analysis from NS1 cells performed as in Figure 1 are shown in Figure 3. Mitochondrial species migrated within the range -1.2×10^{-4} to $-4.3 \times 10^{-4} \text{ cm}^2 \text{V}^{-1} \text{s}^{-1}$. The 25th percentile of fast-migrating species have mobilities within -2.8 to $-4.3 \times 10^{-4} \text{ cm}^2 \text{V}^{-1} \text{s}^{-1}$; the equivalent fraction of slow-migrating species have mobilities within -1.8 to $-1.7 \times 10^{-4} \text{ cm}^2 \text{V}^{-1} \text{s}^{-1}$ (average values,

Table 1). These distributions provide the first detailed description of the electrophoretic mobility of mitochondrial species. These distributions are based on individual measurements and are not compromised by slow detection or broad migration zones.

The observed dispersion in the electrophoretic mobility of mitochondria from NS1 cells is likely the combined result of their natural diversity, the effect of the disruption process used during isolation, and to a lesser degree, interactions with the capillary walls during the separation. The latter problem has been minimized by using poly-AAP-coated capillaries. This hydrophilic coating has been successfully used to reduce protein interactions with the capillary wall.³⁶ We have also used this coating to decrease interactions between liposomes used as mitochondrial models and capillary walls.¹⁷ Without this coating, mitochondria do not migrate within a defined migration window (data not shown).

Application of an electric field to the mitochondrial samples may result in organelle disruption or aggregation.¹⁷ Fortunately, the electric field used in these studies, -200 V/cm , is below the critical fields described in the literature (i.e., 600 V/cm).⁴¹ As discussed above, disruption of cells by nitrogen cavitation decreases the possibility of organelle disruption; thus, the variety of mobilities is likely caused by the disparity of mitochondrial surface properties. There are no reports in the literature about this diversity; however, it is expected that mitochondrial properties will vary throughout the cell cycle, the localization within the cell, the age of the cell, and even cellular performance.

Comparison among Mitochondrial Samples. To use the electrophoretic analysis described above to characterize the electrophoretic mobility of a mitochondrial sample, it is necessary to evaluate the reproducibility of the method. Table 1 contains the electrophoretic mobility data of the same sample analyzed in triplicate from Figure 3. The analysis was performed on the same day to minimize possible error introduced by different sample preparation and instrument set-up. A comparison of the 25th percentile, the median, and the 75th percentile for each analysis indicates that their RSDs are 11, 11, and 4% respectively. These values establish the scope of the method in comparing distributions of electrophoretic mobilities of individual mitochondrial species.

Variations in electrophoretic mobility distributions of mitochondria from different preparations are compared in Figure 4 and Table 1. The mobility distribution of mitochondria from NS1 cells (lower) and CHO cells (upper) are visually different, have a

(41) Zimmerman, U.; Neil, G. *Electromanipulation of Cells*; CRC Press: New York, 1996.

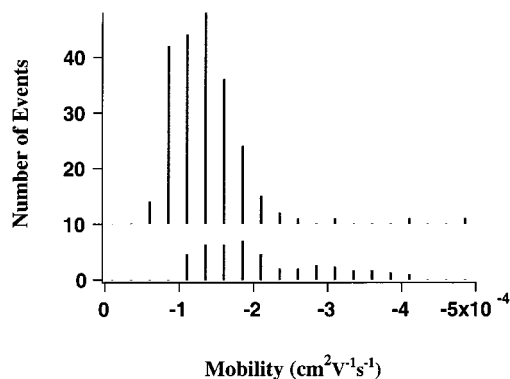


Figure 4. Electrophoretic mobility for mitochondria isolated from NS1 and CHO cells. The upper distribution, vertically offset for clarity, corresponds to CHO cells; the lower distribution corresponds to NS1 cells. Mitochondrial isolation is described in the Experimental Section. CE-LIF experiments are described in Figure 1 for NS1 cells and in the Experimental Section for CHO cells. Data analysis was performed as in Figures 2 and 3.

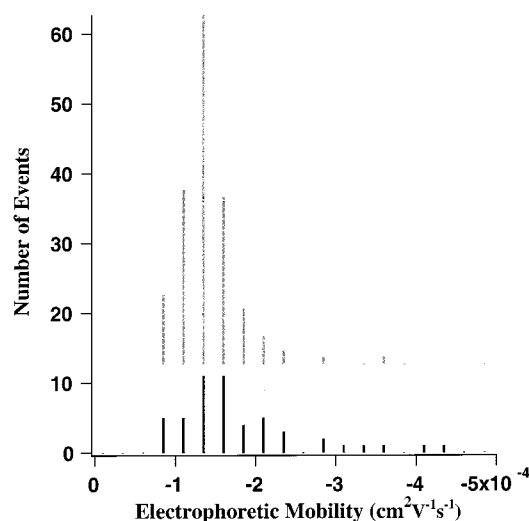


Figure 5. Comparison between high-density and low-density mitochondrial distributions. High-density (1.1079–1.1907 g/mL) and low-density (1.0406–1.1079 g/mL) mitochondria were collected from the Mz 17%/Mz 35% interface (black bars) and the Pc 6%/Mz 17% interface (light bars), respectively. Other conditions were as outlined for Figure 1, and data analysis was performed as outlined in Figures 2 and 3.

different number of events (43 and 157, respectively), and have different electrophoretic characteristics, as seen in Table 1. The most striking difference is above the 75th percentile, where the preparations span the range -2.8 to $-4.3 \times 10^{-4} \text{ cm}^2 \text{ V}^{-1} \text{ s}^{-1}$ and -1.7 to $-4.2 \times 10^{-4} \text{ cm}^2 \text{ V}^{-1} \text{ s}^{-1}$, respectively. Although the differences observed between the distributions of the two mitochondrial preparations may be affected by the use of different isolation and purification procedures, these data clearly indicate that CE-LIF can provide a detailed description of the electrophoretic properties of mitochondrial species.

In a separate experiment, we also determined that the electrophoretic mobility distributions of mitochondria from CHO cells do not seem to differ between fractions containing mitochondria of different density (Figure 5). After mechanical disruption of CHO cells, mitochondria were separated into two density ranges by discontinuous gradient centrifugation: 1.0406–1.1079 g/mL and

1.1079–1.1907 g/mL.³⁵ The light fraction contained 125 events, and the heavy fraction contained 52 events. The relative abundance is consistent with measurements of enzymatic activity by Madden et al.³⁵ A comparison based on a graphic display (not shown) indicates that the slight variations of the mobilities for the different percentiles are insignificant when considering the typical errors shown in Table 1. For example, the electrophoretic mobility range is -0.95 to $-3.6 \times 10^{-4} \text{ cm}^2 \text{ V}^{-1} \text{ s}^{-1}$ and -0.90 to $-5.4 \times 10^{-4} \text{ cm}^2 \text{ V}^{-1} \text{ s}^{-1}$ for the light and heavy fractions, respectively. Similarly, the heavy fraction has slightly higher mobility values at the 25th percentile, the median, and the 75th percentile, namely, -1.3 versus $-1.5 \times 10^{-4} \text{ cm}^2 \text{ V}^{-1} \text{ s}^{-1}$, -1.5 versus $-1.7 \times 10^{-4} \text{ cm}^2 \text{ V}^{-1} \text{ s}^{-1}$, and -1.7 versus $2.2 \times 10^{-4} \text{ cm}^2 \text{ V}^{-1} \text{ s}^{-1}$, respectively. Therefore, we can conclude that the density of a mitochondrion is not related to its electrophoretic mobility. This finding further suggests that electrophoretic mobility and density are orthogonal properties that could be combined for further purification or subfractionation of mitochondrial preparations.

CONCLUSIONS

The distribution of electrophoretic mobilities in a mitochondrial isolate suggests the presence of diversity within mitochondrial preparations, a likely effect of both the preparation procedure and natural diversity. In particular, it has been reported that mitochondria within the cell are a dynamic system, characterized by fission and fusion processes.^{31,32} As a result, it would be expected that their surface properties and, thus, their electrophoretic mobility would be a reflection of that diversity. Considering that individual mitochondrial species can be detected when they migrate out less than 100 ms apart, differences in mobility as low as 400 parts per million are feasible. Thus, electrophoretic distributions promise to be a powerful tool to characterize mitochondrial diversity and may provide the means to characterize or monitor isolation and preparation procedures. The results presented here suggest that individual mitochondria within a specific electrophoretic mobility range could be isolated or further purified after using other isolation techniques such as density gradient centrifugation. The capillary electrophoresis strategy reported for individual mitochondria is likely to be a method easily applicable to other organelles, microsomes, or artificial nanoparticles.

ACKNOWLEDGMENT

This research team is grateful to Dr. Wei-Shou Hu for providing CHO cells, Dr. Sally Palm for providing NS1 cells, Ms. Takia Washington for establishing the cell cultures, Mr. Brent Seager for coating capillaries, and Mr. Hossein Ahmadzadeh for providing acryloylaminopropanol monomer. C.D. thanks the International Union of Biochemistry and Molecular Biology Trust Fund for travel support. R.O.K. thanks Enterprise Ireland. This work was supported by the National Institute of Health (Grant R03 AG18099-01) and by Research Corporation (Grant R10477). K.M.F. acknowledges support from a National Institute of Health Chemistry/Biology Interface Training Grant (Grant GM08700).

Received for review August 22, 2001. Accepted October 16, 2001.

AC010939I